Long Time Series Water Extent Analysis for SDG 6.6.1 Based on the GEE Platform: A Case Study of Dongting Lake

Chunlin Wang, Weiguo Jiang, Yue Deng, Ziyan Ling, and Yawen Deng

***Abstract*—Understanding the variation regularity of water extent can provide insights into lake conservation and management. In this study, inter- and inner-annual variations of water extent during the period of 1987–2020 were analyzed to understand the temporal and spatial distribution characteristics of Dongting Lake. We applied the Multiple Index Water Detection Rule to extract the Dongting Lake water extent quickly and accurately based on Google Earth Engine platform, and then assessed the extraction accuracy. The water surface analysis results showed that (1) based on sustainable development goals (SDG) 6.6.1, the trend of water extent showed the downward fluctuating trend from 1987 to 2020, with the overall average water extent being 1894.48 km². (2) Among the monthly average water area, the largest extent was 2477.14km² (July) and the smallest was 848.14 km² (January). Among the seasonal mean water area, summer was the largest, with an area of 2438.06 km², and winter was the smallest at 967.34 km². (3) For the water inundation frequency, seasonal water bodies accounted for the largest proportion, with 1577.85 km²; the nonwater area was the smallest, with the area of 573.02 km²; and the permanent water area was 1086.21 km². Through the analysis of the historical water body extent of the long time series of Dongting Lake, this study reflected support for SDG, for which the research idea and design can help us understand the importance and feasibility of the SDG 6.6.1 indicator.**

***Index Terms*—Dongting lake, Google Earth Engine (GEE), Landsat, multiple index water detection rule (MIWDR), sustainable development goals (SDG) 6.6.1.**

Manuscript received January 19, 2021; revised April 3, 2021 and May 20, 2021; accepted June 1, 2021. Date of publication June 11, 2021; date of current version January 3, 2022. This work was supported by the National Key Research and Development Program of China under Grant 2017YFB0504102, Grant 2016YFC0503002, Grant 2016YFC0500206, and Grant 2017YFC0506506, in part by the National Natural Science Foundation of China under Grant 42071393 and Grant 41571077, and in part by the NSFC-Guangdong Joint Foundation Key Project under Grant U1901219. The associate editor coordinating the review of this manuscript and approving it for publication Prof. Kaishan Song. *(Corresponding author: Weiguo Jiang.)*

Chunlin Wang, Weiguo Jiang, and Yawen Deng are with the Beijing Key Laboratory for Remote Sensing of Environment and Digital Cities, Faculty of Geographical Science, Beijing Normal University, Beijing 100875, China (e-mail: wangchunlin@mail.bnu.edu.cn; jiangweiguo@bnu.edu.cn; dengywbnu@qq.com).

Yue Deng is with the Beijing Key Laboratory for Remote Sensing of Environment and Digital Cities, Faculty of Geographical Science, Beijing Normal University, Beijing 100875, China (e-mail: dengyue@mail.bnu.edu.cn).

Ziyan Ling is with the Beijing Key Laboratory for Remote Sensing of Environment and Digital Cities, Faculty of Geographical Science, Beijing Normal University, Beijing 100875, China, and also with the School of Geography and Planning, Nanning Normal University, Nanning 530001, China (e-mail: lingziyan@nnnu.edu.cn).

Digital Object Identifier 10.1109/JSTARS.2021.3088127

I. Introduction

THE sustainable development goals (SDGs) are a series of new development goals that are similar to the millennium development goals (MDGs) set by the United Nations. The 17 SDGs are the blueprint for a better and more sustainable future for all, in which SDG 6 is closely related to water and aims to ensure access to water and sanitation for all. Among the goals, SDG 6.6 sets out to protect and restore water-related ecosystems, including mountains, forests, wetlands, rivers, aquifers, and lakes by 2020. In recent years, with the intensification of global warming, water resources have been regarded as an important factor influencing human survival and development, and their changes are receiving great attention. Water-related ecosystems play an important role in the water resource [1], of which, lakes are especially important, as their locations and persistence are both affected by climate and human activity and affect climate biological diversity and human well-being [3]–[5]. Lakes are not only vital resources for industry, agriculture, and domestic water use [7], but they are also considered sentinels of global climate change due to their sensitivity to climatic changes [8]. In the past several decades, many lakes have changed dramatically resulting from water inundation, morphology, and ecology [9]–[13]. Meanwhile, the proposed SDG 6.6.1 monitors changes in the extent of water-related ecosystems over time, focusing on freshwater ecosystems (lakes, etc.) [2]. Therefore, the monitoring of the lake surface water extent will have very important research significance for monitoring SDG 6.6.1 and understanding the law of lake changes and the management of local water resources. Lake surface area is an important parameter for exploring the extent of lake ecosystems; long-time series analyses can also help us to explore the lake's spatiotemporal changes and the impact of climate and human activities in depth.

Remote sensing has the advantages of long-term, large-scale, and high-quality image data, which are suitable for monitoring the dynamic changes of lakes over time by using high-resolution data sources (such as Landsat images, etc.) [14]. It can be well applied to the realization of SDG 6.6.1 and can complete the extent of monitoring. For example, water-related ecosystem' mapping and assessment can be used with remote sensing technology to assess SDG 6.6.1 [1]. Long-time serial water change analysis and flood monitoring are currently research hotspots of remote sensing in hydrology [6]. Besides, Landsat images are widely used in the study of lake surface extent

monitoring because of their long time series, high spatial resolution, and open data storage capacity, which provides us with the possibility of accurately acquiring water area. The high-frequency long-term series data set of global lakes and reservoirs can be constructed to analyze the changes in their water submerged area by using Landsat images [21]. Also, it can be used to extract accurate water extent with a new method [22] and study the spatiotemporal change of lake water extent during the long time series [23]. Therefore, in this study, we used Landsat image data for water extraction research, due to its strong practicality.

Meanwhile, an efficient water extraction method is critical to obtaining accurate water surface extent from remote sensing images [24]. The water index followed by a threshold was widely used to extract surface water body for its convenience [25]. At present, the most widely used water body indexes include the normalized differential water index (NDWI), the modified NDWI (MNDWI) [26], [27]. What's more, there is also an automatic water extraction index (AWEI) that can be used to extract water bodies, which included two kinds of indexes, $\mathrm{AWEI_{nsh}}$ and $\mathrm{AWEI_{sh}}$. [28]. $\mathrm{AWEI_{nsh}}$ is an index formulated to effectively eliminate nonwater pixels, including dark built surfaces in areas with urban backgrounds and $\mathrm{AWEI_{sh}}$ is primarily formulated for further improvement of accuracy by removing shadow pixels that $\mathrm{AWEI_{nsh}}$ may not effectively eliminate [28]. However, an ideal single threshold to distinguish between water bodies and nonwater bodies is difficult to determine because the spectral signature of a water body varies in space and time [25]. We aim to extract the water surface extent of Dongting Lake in the Yangtze River Basin (YRB) through a relatively simple, fast, and accurate method, so this study extracts the water area of Dongting Lake with a new water detection rule developed by Deng *et al.* [14]. This detection rule is called the multiple index water detection rule (MIWDR), which has been proven to obtain high extraction accuracy in the YRB, and the water extraction process was simple and convenient.

However, traditional studies of the water body (lake surface area) usually used fewer images during a specified period for study regions [15], which had brought great challenges to the research on the changing extent of the water body with a high frequency and long time series because of the difficult process with vast remote sensing images. In recent years, a platform called Google Earth Engine (GEE) has been developed to facilitate large-scale analysis of geospatial data and processing of remote sensing big data [16], [17]. Therefore, the long time series dynamic lake extent monitoring research based on the GEE cloud platform will become the direction of future water body studies and has some excellent achievements. Based on the GEE platform, the mapping of long-term global open-surface water bodies from 1984 to 2015 [18], the spatiotemporal changes of open-surface water bodies in the contiguous United States from 1984 to 2016 [19], and the long-term evolution of the Mongolian plateau lake and its spatial and temporal distribution characteristics [20] had been completed. Therefore, the GEE provides us with a new insight to understand the long-term changes in the lake surface area. The MIWDR by using Landsat images was based on the GEE platform, which provides an excellent opportunity for monitoring the Dongting Lake with the advantages of long time series remote sensing data.

Dongting Lake is the second-largest freshwater lake in China and also the largest throughput lake, which has a strong storage capacity and is also a typical river-connecting lake that interacts with the Yangtze River [30], [31], thus forming a complicated relationship between river and lake. Dongting Lake is also an important natural water resource in the YRB, with many important functions such as water supply, irrigation, climate regulation, etc. During recent decades, the water body of the Dongting Lake surface has undergone a remarkable spatiotemporal change that has resulted in significant hydrological, ecological, and economic consequences [32], [33], [41]. Therefore, Dongting Lake has fluctuated a lot mainly due to intensive human activities and the change of climate. Numerous studies have demonstrated that the hydrological environment of Dongting Lake has changed after the operation of the Three Gorges Dam (TGD), especially the variations in water surface [29], [45]. According to statistics of Hunan Provincial Water Resources Department, four severe droughts occurred in Dongting Lake during 2000–2010 (in 2000, 2002, 2005, and 2006, respectively) [43]. What's more, the relationship between water surface extent and anthropogenic or climatic factors keeps still unclear in Dongting Lake. Consequently, the water body surface extent change of Dongting Lake has received considerable scientific attention. Some researchers monitored the dynamic water extent change through MODIS images [42], derived the relationship between water level and water area of Dongting Lake and obtained the history and real-time water area change [34], [46]. Meanwhile, the relationship between inundation frequency and wetland vegetation change, the inundation pattern also have been concerned by scholars [35]–[37]. However, in the study of Dongting Lake, there are still some problems, such as the short time series of remote sensing data, the low accuracy of water area, and the lack of in-depth study of spatiotemporal characteristics [41], [42], [46].

The purpose of this study is:

1) to quickly and accurately extract the water surface extent of Dongting Lake based on the GEE platform;

2) to study the extent change of Dongting Lake from 1987 to 2020 for SDG 6.6.1;

3) to analyze the spatiotemporal characteristics of the Dongting Lake extent and discuss the causes of changes in Dongting Lake.

II. Materials and Methods

A. Study Area

This study area was in the Dongting Lake (28°30'N–30°20'N, 111°40'E-113°10'E), the second-largest freshwater lake in China, which is located on the southern bank of the middle and lower reaches of the YRB and spans Hubei and Hunan provinces. It is fed by four rivers, including Xiangjiang, Zishui, Yuanjiang, and Lishui and has three major estuaries (Ouchi, Songzi, and Taiping) of the Yangtze River (see Fig. 1) [38]. It is directly connected to the Yangtze River, forming a close relationship between rivers and lakes, which is also an important fluctuating

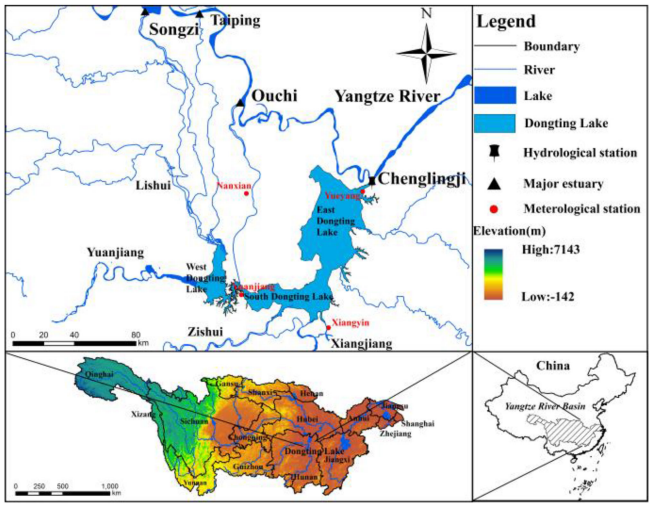

Fig. 1. YRB and the location of Dongting Lake. Four rivers feed the Dongting Lake (Xiangjiang, Zishui, Yuanjiang, and Lishui) and three estuaries (Ouchi, Songzi, and Taiping) are also shown.

lake and international wetland in the middle and lower reaches of the Yangtze River in China [44]. The water of the entire lake finally discharges into the Yangtze River through the Chenglingji hydrological station [39], which is also related to the fact that the topography of Dongting Lake is high in the south and west, low in the north and east. The subtropical monsoon climate is typical in this area, in which the summer is hot and rainy, winter is mild with little rain, and the dry and wet seasons are distinct. April to September is defined as the wet season, with precipitation accounting for more than half of the total annual precipitation (AP), and the surface area could be more than 2000 km^2. October to March is defined as the dry season, and the surface area is typically < 1000 km^2 due to the reduced rainfall. With the evolution of the hydrology and morphological characteristics of Dongting Lake water, which is gradually divided into three parts: East Dongting Lake, West Dongting Lake, and South Dongting Lake.

B. Long Time Series Landsat Data

In this study, Landsat images were used to extract water extent of Dongting Lake and were processed on the GEE platform, which used all available Landsat 5, 7, and 8 surface reflectance images of the entire Dongting Lake from 1987 to 2020 [see Fig. 2(a)], in which the path/row is 123/40 and 124/40. The total number of these images was 783 scenes. Then, image mosaic and clipping and the extraction of the water body are carried out on the GEE platform. After those, we selected the effective water body images for analysis.

Since the Landsat image of a scene cannot cover the Dongting Lake, we will acquire images within one month for mosaics to obtain a completed image of Dongting Lake. After the mosaic and clipping were completed, the water body extraction process was carried out based on the new MIWDR. Then, we used visual inspection to select the data with cloud cover small enough not to affect the analysis of the Dongting Lake water surface. As shown in Fig. 2(b), the images with effective water body were

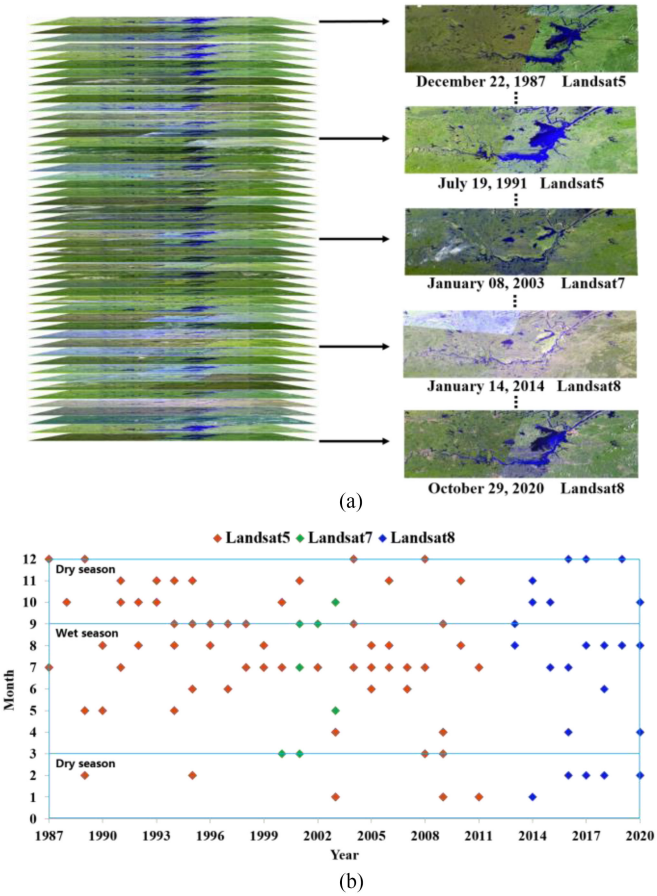

Fig. 2. Remote sensing image data: (a) Landsat images of Dongting Lake. (b) Number of effective water body scenes per month per year.

89 (33 from dry season and 56 from wet season). The maximum of images were from July (15 scenes) and the minimum from March and April (3 scenes). Finally, the effective water data set of Dongting Lake was constructed.

C. Climate and Other Ancillary Data

In this study, AP, monthly precipitation (MP), annual mean temperature (AMT) and Joint Research Centre of European Commission (JRC) Monthly Water History (v1.2) data[1] [18], and global water dataset which was created by Pickens et al. [50][2] datasets were used to analyze the possible factors and accuracy assessment on water surface extent for Dongting Lake.

Precipitation and temperature data (1987–2019) from four stations (stations of Nanxian, Yuanjiang, Xiangyin, and Yueyang) around Dongting Lake was acquired from China Meteorological Administration and was used to analyze the effects of rainfall and temperature on the water surface of Donting Lake. In this study, AP and MP used the total average value of four stations for each year and AMT used the mean temperature value of four stations (see Fig. 3).

[1][Online]. Available: https://esdac.jrc.ec.europa.eu/

[2][Online]. Available: www.glad.umd.edu/dataset/global-surface-water-dynamics

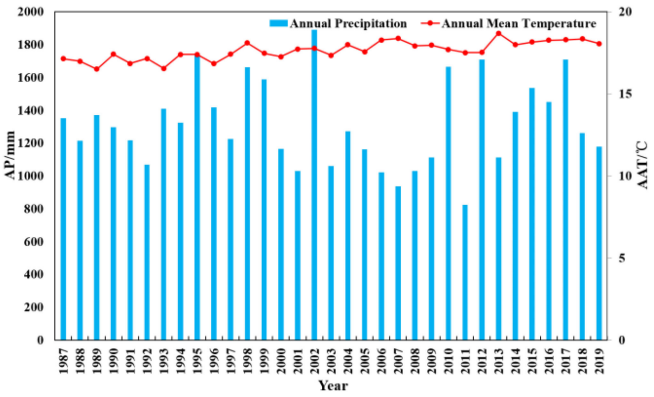

Fig. 3. Dongting lake climate data used in this study.

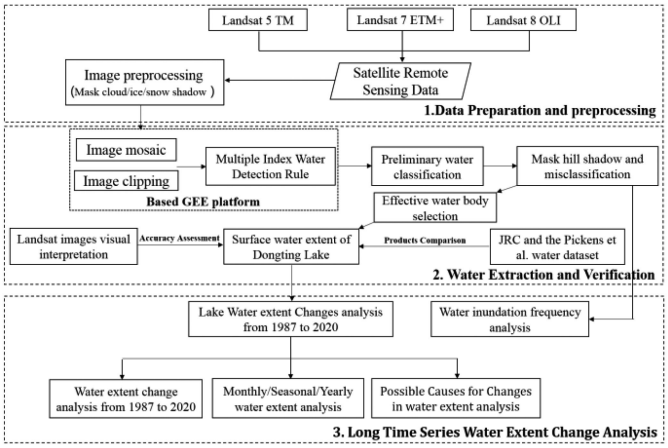

Fig. 4. Flowchart of this study: 1. data preparation and preprocessing, 2. water extraction and verification, and 3. long time series water extent change analysis.

The JRC Monthly Water History (v1.2) dataset and global water dataset (the Pickens *et al*. [50]) were used as ancillary data to compare the results of water extraction based on MIWDR [18]. These data can be accessed through the GEE platform. In addition, shuttle radar topography mission digital elevation model data were collected to display the elevation in the YRB.

D. Methodology and Flowchart

1) Flowchart: The flowchart of analyzing the lake surface in this study is displayed in Fig. 4. It mainly consists of three parts: The first part mainly introduces the remote sensing data of this study and the image preprocessing. The second part mainly introduces the water extraction process on the GEE platform, and finally obtains effective water body results through verification. The third part mainly analyzes the long time series water extent change and possible causes for it. The details are described in the following sections.

2) Multiple Index Water Detection Rule: The water extraction method used in this study was mainly based on the new MIWDR proposed by Deng *et al.* [14], which processed all three Landsat optical payloads images to investigate the long-term changes of open-surface water bodies and it had a higher extraction accuracy when extracting water bodies in the YRB. This method mainly used NDWI, AWEI, NDVI, and EVI and other comprehensive indexes to target for each pixel, if the pixel met the following conditions: if ($\omega = 1$) and ($\mathrm{AWEI_{nsh}}$ - $\mathrm{AWEI_{sh}}$> -0.1) and (MNDWI> NDVI or MNDWI> EVI), it would be classified as a water body, and if it was not satisfied ($\omega = 0$), it would be classified as a nonwater body. The specific operation of the method was described as follows: First, the quality bands product of the Landsat surface reflectance product was generated according to the F-mask algorithm and then masked for the cloud, cloud shadow, and snow. Then, the images are classified according to the above conditions to obtain the initial water distribution in the Dongting Lake inundation area and then compared with the JRC global surface water occurrence layer to remove mountain shadows and misclassified pixels. The mathematical expression of this condition is as follows:

$$\mathrm{MNDWI} = (\rho_{\mathrm{green}} - \rho_{\mathrm{NIR}}) / (\rho_{\mathrm{green}} + \rho_{\mathrm{NIR}}) \quad (1)$$

$$\mathrm{NDVI} = (\rho_{\mathrm{NIR}} - \rho_{R}) / (\rho_{\mathrm{NIR}} + \rho_{R}) \quad (2)$$

3) Water Inundation Frequency: The water inundation frequency (WIF) refers to the ratio of the number of times a region is submerged in water within a certain time to the total times of inundation. In this study, the frequency of water inundation is calculated by the proportion of each pixel in all the raster images of water pixels. The calculation formula can be described as

$$\mathrm{WIF} = \frac{\sum_{i=1}^{N} w}{N} \times 100\% \quad (7)$$

where N represents the number of available water body image layers in the observation period, ω represents a binary variable ($\omega = 1$ indicates water body and $\omega = 0$ indicates non-water body). WIF ranges from 0 to 100%. According to the definition of WIF and other scholars' study method, water bodies were classified with WIF greater than 75% as permanent water bodies, less than 25% water bodies as nonwater bodies, and the remaining water body types as seasonal water bodies [15], [19].

In addition, we regard the maximum and minimum water extent as the corresponding maximum and minimum water extent when WIF > 0 in different time scales.

4) Long Time Series Trend Analysis: Mann-Kendall (MK) test [47], [48], a nonparametric statistic test method, requires that the samples do not have to follow a specific distribution, and the test results are not disturbed by a few outliers. It can accurately reveal the trend of time series and is suitable for trend analysis of nonnormally distributed data series such as hydrology and meteorology, which has been widely used. MK test is based on the statistic S defined as follows:

$$S = \sum_{i=1}^{n-1} \sum_{j=i+1}^{n} sgn\,(x_j - x_i) \quad (8)$$

where x_j and x_i represent the values at time i and j, respectively. $sgn(x)$ is the symbolic function. It has been reported that the statistic S is approximately normally distributed when n ≥ 10. The variance of S was calculated by the following:

$$\mathrm{Var}\ (S) = \frac{n\,(n-1)\,(2n+5)}{18}. \quad (9)$$

The standard normal test statistic Z_s is computed at

$$Z_s = \begin{cases} \frac{S-1}{\sqrt{\mathrm{Var}(S)}}, & S > 0 \\ 0, & S = 0 \\ \frac{S+1}{\sqrt{\mathrm{Var}(S)}}, & S < 0 \end{cases}. \quad (10)$$

Positive values of Z_s indicate increasing trends while negative Z_s values show decreasing trends. Testing trends is done at the specific α significance level. When $|Z_s| > \mathrm{Z}_{1-p/2}$, the null hypothesis is rejected and a significant trend exists in the time series. $\mathrm{Z}_{1-p/2}$ is obtained from the standard normal distribution table. In this study, significance levels $p = 0.05$ were used. At the 5% significance level, the null hypothesis of no trend is rejected if $|Z_s|$>1.96.

5) Water Extraction Verification: In this study, we aimed to explore whether the water extraction results were reliable [49]. This study verified the accuracy through the comparison with the actual Landsat image visual interpretation results and MIWDR-based water body extraction results. First, randomly select sample points were created (in this study, 300 random sample points are selected in the Dongting Lake area), through visual interpretation in Landsat images, which were classified into nonwater bodies and water bodies, and then a confusion matrix was established with the water body extraction results at the corresponding time. The final accuracy evaluation result was analyzed through overall accuracy and kappa coefficient.

What's more, this study also used this method that comparison and analysis of the water extraction results with the existing Dongting Lake water dataset. The JRC Global Surface Water Dataset and the Pickens *et al*. [50] dataset of Dongting Lake are the current water dataset. We used the relative error to calculate the accuracy between the extracted water area and water dataset area. We used the following formula to calculate the relative error:

$$R = \left(\frac{|S_a - S_e|}{S_e} \right) \times 100\% \quad (11)$$

where *R* is the relative error between the water area of the extracted and the water dataset, S_a is the area of the water dataset area, and S_e is the area of the extracted water area.

III. Results

A. Water Extent Changes of Dongting Lake From 1987 to 2020, for SDG 6.6.1 Monitoring

The overall water extent changes of Dongting Lake had distinct intra- and inter-annual characteristics during the period of 1987–2020. As shown in Fig. 5(a), the long time series of the water extent changes showed a significant fluctuation downward trend from 1987 to 2020 ($Z_s = -2.073, p < 0.05$). SDG Indicator 6.6.1 focuses on the change in the extent of water-related ecosystems over time. Therefore, through the analysis of water extent, the maximum water extent of Dongting Lake was 3060.30 km², which occurred on July 06, 1998, and the minimum water extent was 524.09 km², which occurred on January 14, 2014, from 1987 to 2020 [see Fig. 5(a)]. Through the analysis of maximum and minimum water extent, the overall range was 2493.08 km², and the average water extent of Dongting Lake was 1858.38 km². Fig. 5(b) shows the spatial water extent of the maximum and minimum in this study. All of them fully showed that the water extent changes of Dongting Lake had obvious inter-annual and intra-annual characteristics, which was a typical seasonally changing lake.

B. Monthly Water Extent Analysis of Dongting Lake From 1987 to 2020

As the water extent of Dongting Lake had obvious intra-annual change characteristics, which was analyzed through the monthly water statistics, Fig. 6 shows the monthly minimum, maximum water area data, the corresponding occurrence year, and the average water area. Among the monthly mean water area, the largest was 2477.14 km² (July), and the smallest was 848.14 km² (January). Among the monthly maximum water area, the largest area was 3060.30 km², which occurred in July, 1998 and the smallest was 1145.61 km², which occurred in January, 2003. Among the monthly minimum water area, the largest area was 1994.58 km², which occurred in June, 2018 and the smallest was 524.09 km², which occurred in January, 2014. It can be seen that the monthly water area is larger in June, July, and August, while January is the smallest.

Between April and September of the wet season, the monthly maximum water area was >2000 km² and sometimes even reached >3000 km² and the monthly minimum water area was >1000 km² and the average area was >1000 km². Between October and March of the dry season, the monthly maximum water area was mostly <1500 km² and the monthly minimum water area was all <1000 km² except October and the average area was approximately 1000 km² mostly. In summary, from January to March, the water area was in the lowest period of the year. From April to June, the water body area increased significantly. From July to September, the water area was at its maximum value in a year. From October to December, the water body area had a significant decreasing trend.

Likewise, Fig. 7 shows the minimum and maximum water spatial extent of Dongting Lake for each climatological month during a 34-year period. The monthly minimum and maximum

$$\mathrm{EVI} = 2.5 \times (\rho_{\mathrm{NIR}} - \rho_R) / (\rho_{\mathrm{NIR}} + 6 \times \rho_R - 7.5 \times \rho_{\mathrm{blue}} + 1) \quad (3)$$

$$\mathrm{AWEI}_{nsh} = 4 \times (\rho_{\mathrm{green}} - \rho_{\mathrm{SWIR}}) - (0.25 \times \rho_{\mathrm{NIR}} + 2.75 \times \rho_{\mathrm{SWIR2}} \quad (4)$$

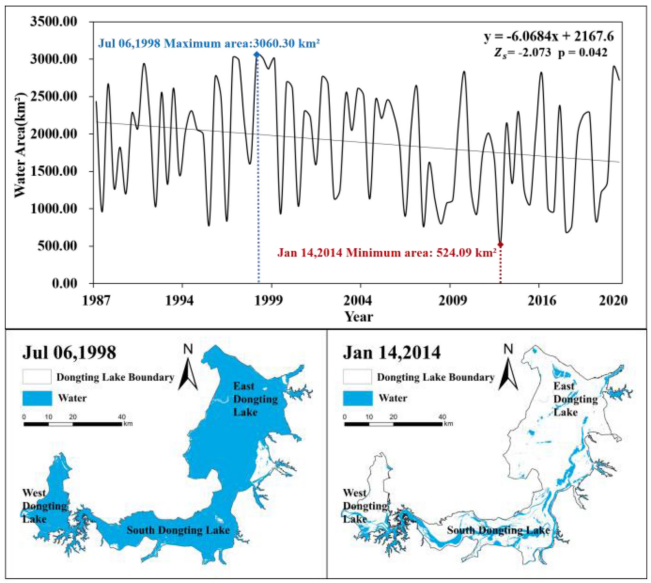

Fig. 5. Variations in the water area of Dongting Lake during 1987–2020. (a) Long time series water area changes during 1987–2020. (b) Maximum and minimum water extent of Dongting Lake in this study.

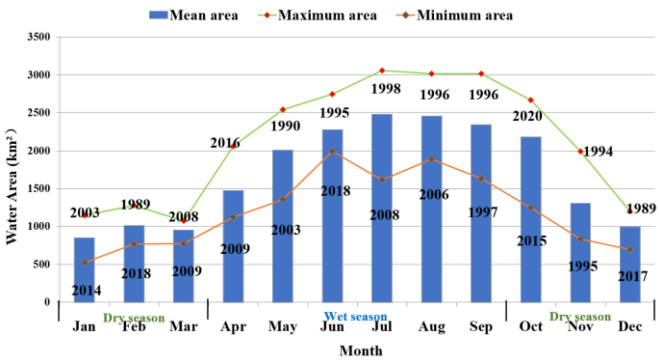

Fig. 6. Monthly maximum, minimum, and mean water area in Dongting Lake from 1987 to 2020 (The number on the line is the corresponding year of occurrence).

water extent of each month was consistent with the statistical data and both showed obvious seasonality characteristics.

The monthly maximum water extent between May and October was more than double that between December and February. Especially, from June to September, most (>50%) of Dongting Lake was inundated even at minimal water extent except for some tributary exits and some areas with higher terrain. During these months, the narrow water outlet in the northeast and most of the internal lakes were always connected.

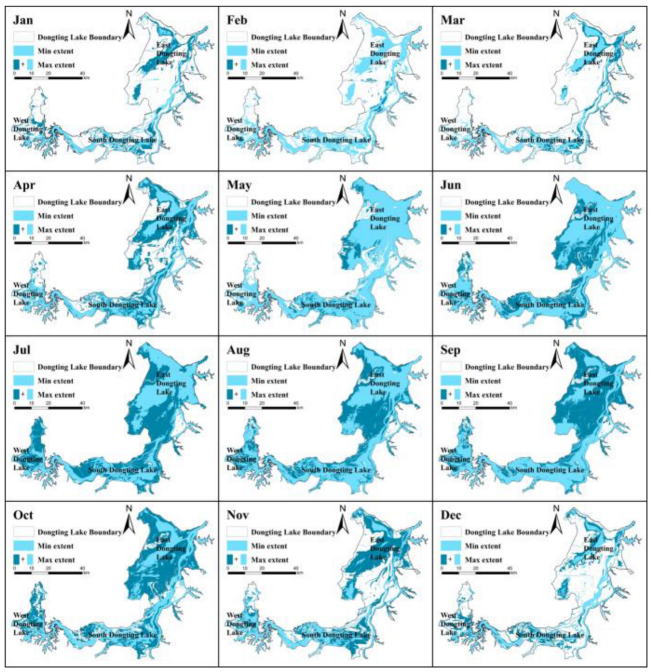

Fig. 7. Monthly maximum and minimum water extent in Dongting Lake during 1987–2020.

However, when the monthly minimum water extent occurred between October and March with an inundation area <1500 km^2, the water of Dongting Lake only retained some main permanent lakes and the overall water body distributed in stripes, which was divided into some sections. Likewise, the monthly maximum water extent was significantly smaller during December–February than other months.

C. Seasonal Water Extent Analysis of Dongting Lake From 1987 to 2018

In this study, calendar months divide March–May into spring, June–August into summer, September–November into autumn, and December–February into winter. The analysis result of water changes of Dongting Lake showed obvious seasonal variation characteristics. As shown in Fig. 8, the seasonal water area of summer and autumn were larger than that of spring and winter overall. Among the seasonal maximum water area, summer was the largest at 3060.30 km², and the smallest was in winter at 1239.53 km². Among the seasonal minimum area, summer is the largest at 1616.22 km², and winter is the smallest at 767.99 km². Among the seasonal mean area, summer was the largest at 2438.06 km², and winter was the smallest at 967.34 km².

$$\mathrm{AWEI}_{sh} = \rho_{\mathrm{blue}} + 2.5 \times \rho_{\mathrm{green}} - 1.5 \times (\rho_{\mathrm{NIR}} + \rho_{\mathrm{SWIR1}}) - 0.25 \times \rho_{\mathrm{SWIR2}} \tag{5}$$

$$\omega = \begin{cases} 1 & (\mathrm{AWEI}_{nsh} - \mathrm{AWEI}_{sh} > -0.1) \text{ and } (\mathrm{MNDWI} > \mathrm{NDVI} \text{ or } \mathrm{MNDWI} > \mathrm{EVI}) \\ 0 & \text{else} \end{cases}. \tag{6}$$

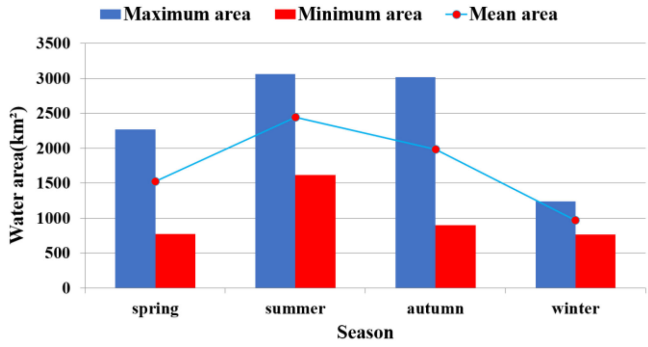

Fig. 8. Seasonal maximum, minimum, and mean water area in Dongting Lake during 1987–2020.

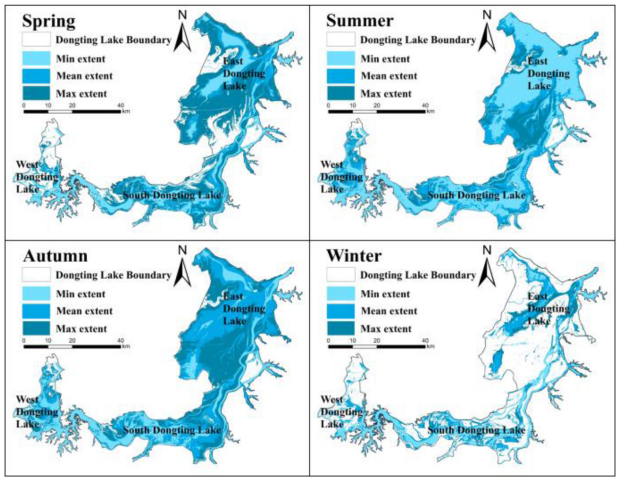

Fig. 9. Seasonal maximum, minimum, and mean water extent during 1987–2020.

The water body area is larger in summer and autumn, followed by spring, and the overall water body area is the smallest in winter. Likewise, it can be seen from Fig. 9 that the water spatial distribution of different seasons, which was basically the same as Fig. 8. The water extent of summer can cover the most proportion of Donting Lake main district, but the water extent of winter only took up the small part with the shape of stripe. The variation characteristics of seasonal water areas were mainly related to the changes in the flood season and rainfall in the YRB.

To further study the seasonal trend of Dongting Lake water surface, the regression analysis of the water body area in each season was conducted. The constant in the equation represents the base of the water surface area, and the slope represents the rate of decline of the water surface area of Dongting Lake. The larger the absolute value of the slope, the more obvious the downward trend.

According to the trend chart of each season (see Fig. 10), the water area of each season showed a downward trend, in which the water surface area declined fastest in spring [see Fig. 10(a)], followed by autumn [see Fig. 10(c)], summer [see Fig. 10(b)], and the winter water surface area [see Fig. 10(d)] declined slowest. Overall, the downward trend in summer and autumn was lower than that in spring and winter, which was also consistent with the long time series water change characteristics.

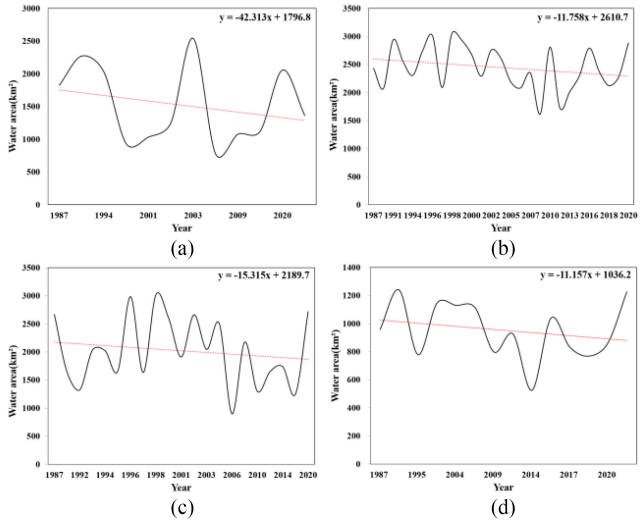

Fig. 10. Variation trend of water area in (a) spring, (b) summer, (c) autumn, and (d) winter during 1987–2020.

D. Yearly Water Extent Analysis of Dongting Lake From 1987 to 2018

The purpose of SDG 6.6.1 is to promote the protection and governance of the water resource through monitoring of water extent over time. Figs. 11 and 12 present annual maximum and minimum water extent from 1987 to 2020, which showed obviously inter-annual variability across the panels. As shown in Fig. 11, when the annual maximum water extent occurred, most inundated areas were connected, forming a large lake water body for each year, which covered closed to the full Dongting Lake area, but it varied greatly from year to year. From 1987 to 2003, the maximum water area showed an upward trend, which reached the largest value in 1998. After 2003, the maximum water body area changed with large fluctuations, especially in 2008 and 2011, with the area $<$ 2000 km². In recent years, the maximum area has been relatively stable. The maximum water in each year mainly occurred around the summer months, of which the time of occurrences was higher in July and August. However, the annual minimum water extent (see Fig. 12) shows fluctuating characteristics from 1987 to 2003, reaching a maximum in 1994. Since 2003, the minimum water area has been declining rapidly. Especially in 2014, the water body only covered a small part of the main channel area.

From the mean water area for each year (see Fig. 13), the water inundation area of Dongting Lake shows a trend of significant decreasing fluctuations (Z_s= -2.433, $p = 0.015 < 0.05$). From 1987 to 2020, the water area of Dongting Lake was divided into three periods according to important events (see Fig. 13). First, the TGD was established and operated stably in 2003. Therefore, the first period was from 1987 to 2002. During this period, the overall water area showed an upward trend (Slope = 39.007) and reached the maximum value (3038.74 km²) of the water area around 1998, which may be related to the outbreak of major floods in China that year. Therefore, Dongting Lake was in an expansion state during this period. Then, the water area showed a rapid downward trend (Slope = -57.055) from

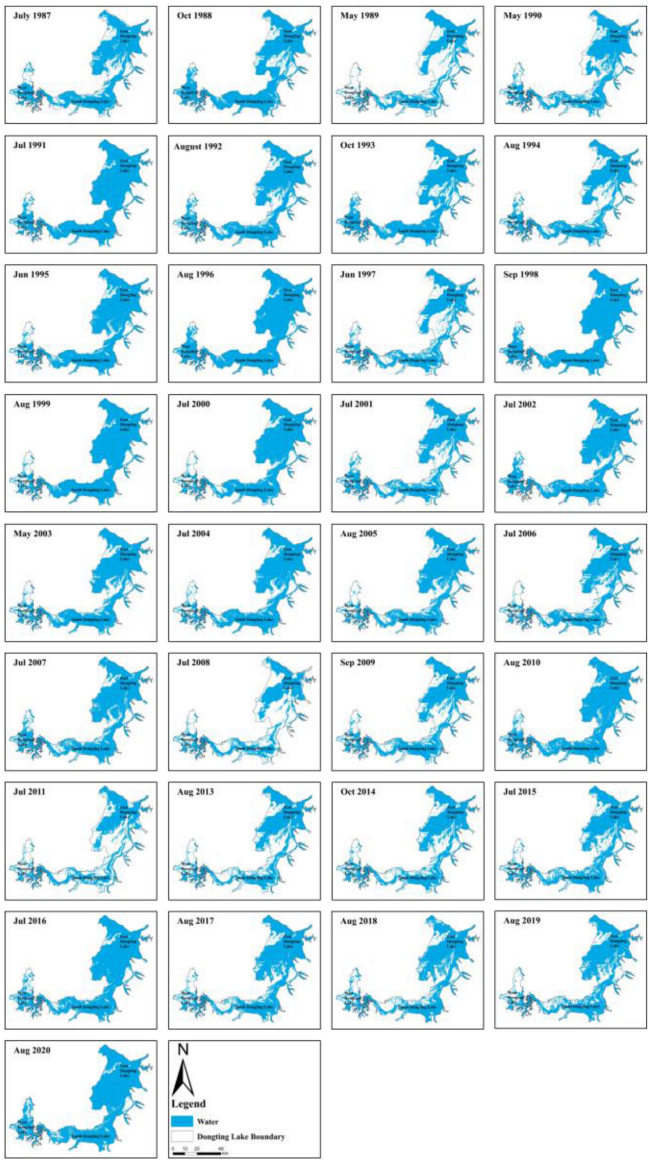

Fig. 11. Maximum water extent for each year during 1987–2020.

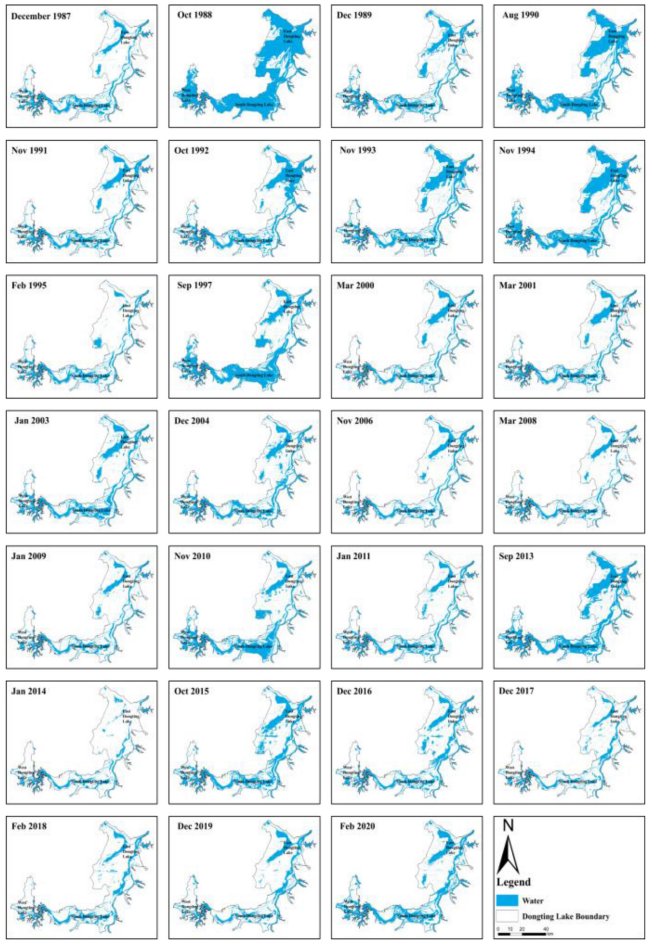

Fig. 12. Minimum water extent for each year during 1987–2020.

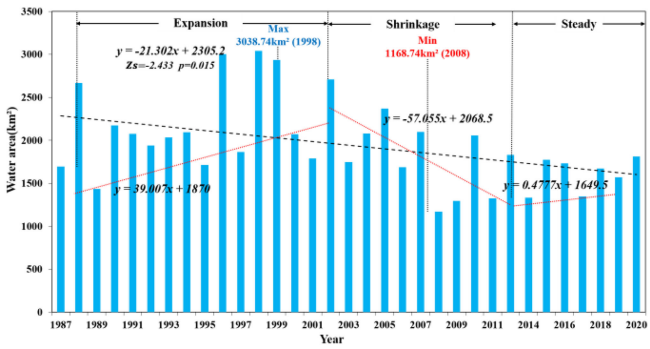

Fig. 13. Mean water area changes in Dongting Lake for each year from 1987 to 2020 .

2003 to 2014, which may be related to the storage of the TGD after 2003. During this period, the water area declined to the minimum value in 2008 (1168.74 km²). Therefore, Dongting Lake was in a shrinkage state. In 2014, the Chinese government began to increase the ecological protection of the Dongting Lake area and set up the Ecological Economic Zone to promote the protection of local water resources. Finally, from 2015 to 2020, the water area was in a stable rising distribution state (Slope = 0.4777), which compared with the previous stage, the water area was at a lower level in the entire time series, with the area of around 1800 km².

E. WIF Analysis of Dongting Lake From 1987 to 2020

According to the SDG 6.6.1, we used WIF to analyze the spatial extent changes of Dongting Lake from 1987 to 2020. Meanwhile, in order to better analyze the changes in the frequency of inundation of water bodies in different stages, reveal the law of temporal and spatial changes of water bodies in different stages. According to the three stages of Dongting Lake we have divided, we got the frequency of water inundation in different periods and the distribution of different types of water bodies. Fig. 14 presents the Dongting Lake spatial distribution patterns during different periods. The WIF illustrated the spatial distribution of the count of inundation times as a percentage of the total times during different periods. The darker red color indicates a lower inundation frequency, and the darker blue color indicates a larger inundation frequency. Fig. 14(a)–(c) of

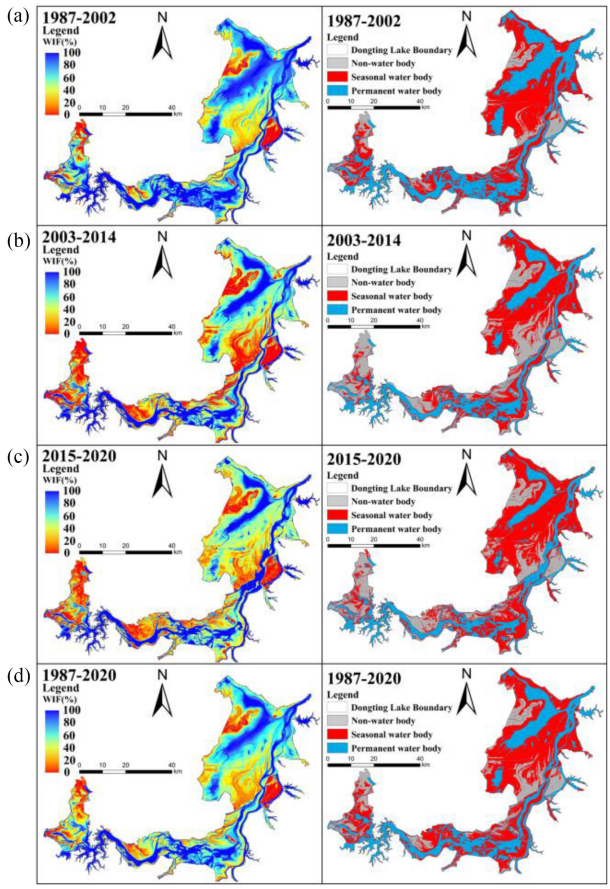

Fig. 14. WIF map of different periods (left column) and the corresponding different water bodies extent distribution map (right column) during 1987–2020.

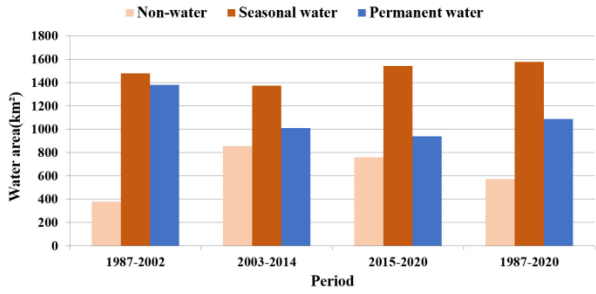

Fig. 15. Different water body type areas in Dongting Lake during different periods.

left column, demonstrating the WIF of Dongting Lake in three periods, can see the inundation frequency and high-value areas in the expansion period of 1987–2002 was higher and larger than other periods, with an average inundation frequency of 63.81%. However, by the degradation period of 2003–2014, the low-value areas had increased significantly, with the high-value areas concentrated in the center of the lake and the average inundation frequency of 50.31%. During the steady period from 2015 to 2020, the average WIF was 48.40% because the water area had dropped to a lower level. The spatial pattern of the multiyear mean inundation frequency [the left row of Fig. 14(d)] shows that most areas of the higher frequency (nearly 60–90%) was distributed near river channels or sub-lakes in Dongting Lake, because the inundation in the lake always began with high discharges in the river channels. Likewise, the alluvial regions of the lake (mainly in the north in West Dongting Lake) had an obviously lower inundation frequency than other regions. Additionally, judging from the distribution of water bodies during different periods, the seasonal water area (the inundation frequency of 25 to 75%) was mostly distributed and mainly concentrated in the East Dongting Lake and South Dongting Lake. The area of permanent water was distributed in the center of lake channels and the nonwater body was on the edge area of the lake.

Fig. 15 shows the area of various water bodies of Dongting Lake in different periods. According to the water body area statistics, the overall total area of Dongting Lake was 3237.08 km², of which the permanent water area was 1086.21 km², accounting for 33.56%; the seasonal water area was 1577.85 km², accounting for 48.74%; and the nonwater area was 573.02 km², accounting for 17.70% during 1987–2020. The seasonal water area accounted for nearly half of the Dongting Lake area, which also fully showed seasonal inundation variation characteristics and was consistent with the previous analysis result. The area of nonwater body was the smallest during 1987–2002, at 378.34 km², and the largest during 2003–2014, at 855.04 km². The seasonal water body was the largest during 2015–2020 at 1541.91 km² and the smallest during 2003–2014 at 1373.63 km². The permanent water body was the largest during 1987–2002 at 1379.77 km² and the smallest during 2015–2020 at 936.95 km². Additionally, the area of nonwater body showed a trend of first increasing, then decreasing, however, to which the trend of seasonal water body changes is contrary. Additionally, the area of permanent water body showed a continuous decrease trend from 1987 to 2020.

IV. Discussion

A. Water Verification of Extraction Result

In this study, we generated 300 random sample points at first, next spaced them evenly within the Dongting Lake area, and then selected 9 images of different years and different periods from 89 effective water images. After that, the accuracy of the water extraction result was evaluated with the corresponding Landsat images.

Table I showed the accuracy of water extraction result of Dongting Lake. The average overall accuracy and kappa coefficient were 93.15% and 0.83, respectively, which indicated that the extraction water results had better accuracy and can be used to further analyze. In addition, judging from the accuracy evaluation results, the water extraction effect of each period had little difference. Therefore, there are no inconsistencies in the extraction water extent by the three sensors and it had no difference influences on the analysis of the historical water extent through three Landsat optical payloads.

Besides, the water extraction results in this study were also compared with the JRC water dataset and the Pickens *et al.* [50] dataset for Dongting Lake to calculate the overall accuracy,

TABLE I
CONFUSION MATRIX FOR ACCURACY ASSESSMENT IN THIS STUDY

Time	Samples	Landsat images		Total	Accuracy
August,1994		Water body	Non-water body		
MIWDR	Water body	196	18	214	Overall Accuracy = 92.67% Kappa coefficient = 0.83
	Non-water body	4	82	86	
	Total	200	100	300	
September,1996		Water body	Non-water body	Total	Accuracy
MIWDR	Water body	257	16	273	Overall Accuracy = 94.00% Kappa coefficient = 0.70
	Non-water body	2	25	27	
	Total	259	41	300	
July,2001		Water body	Non-water body	Total	Accuracy
MIWDR	Water body	182	23	205	Overall Accuracy = 94.00% Kappa coefficient = 0.70
	Non-water body	3	92	95	
	Total	185	115	300	
April,2003		Water body	Non-water body	Total	Accuracy
MIWDR	Water body	102	13	115	Overall Accuracy = 90.00% Kappa coefficient = 0.79
	Non-water body	17	168	185	
	Total	119	181	300	
June,2007		Water body	Non-water body	Total	Accuracy
MIWDR	Water body	174	19	193	Overall Accuracy = 96.33% Kappa coefficient = 0.84
	Non-water body	4	103	107	
	Total	178	122	300	
January,2009		Water body	Non-water body	Total	Accuracy
MIWDR	Water body	69	6	75	Overall Accuracy = 92.33% Kappa coefficient = 0.90
	Non-water body	5	220	225	
	Total	74	226	300	
October,2014		Water body	Non-water body	Total	Accuracy
MIWDR	Water body	183	10	193	Overall Accuracy = 95.67% Kappa coefficient = 0.91
	Non-water body	3	104	107	
	Total	186	114	300	
February,2016		Water body	Non-water body	Total	Accuracy
MIWDR	Water body	85	11	96	Overall Accuracy = 95.33% Kappa coefficient = 0.89
	Non-water body	3	201	204	
	Total	88	212	300	
August,2019		Water body	Non-water body	Total	Accuracy
MIWDR	Water body	190	25	215	Overall Accuracy = 90.67% Kappa coefficient = 0.79
	Non-water body	3	82	85	
	Total	193	107	300	

kappa coefficient. As shown in Table II, the overall effect of the water extraction results was satisfying, where the overall accuracy are all more than 85% and the average value is 93.33% and 89.67% through the comparison with the Joint Research Centre of European Commission and Pickens *et al.*'s [50] dataset. In addition, the comparison results also show that the average values of Kappa coefficients are 0.85 and 0.76, respectively.

From the perspective of relative error, comparing the area of the water extraction results in this study with the two water data sets, the overall relative error is less than 10%. From the comparison results of different data sets, the relative error value in the area comparison results between the JRC data set and the water body extraction results in this study is low and most of them are less than 5%. Compared with the water results of this study, the relative error values of the Pickens *et al*. [50] were higher, and some even higher than 5%. But overall the relative error was small, and the extraction accuracy was also high. The above results all showed that the water body results extracted based on MIWDR are highly consistent with the current water body datasets.

In general, although the water verification results in different months are different, the overall water extraction effect is suitable for the long time series analysis study for Dongting Lake.

B. Possible Causes for Changes in Water Area of Dongting Lake

Due to the complicated relationship between Dongting Lake and the Yangtze River, the human activities in the YRB and around the Dongting Lake have a large impact on the water area

TABLE II
ACCURACY ASSESSMENT AND AREA COMPARISON BETWEEN WATER EXTRACTION AREA AND JRC, PICKENS' WATER DATASETS

Time	Water Extraction area Based on MWIDR(km²)	JRC Monthly Dataset				The Pickens et al [50] Monthly Dataset			
		Overall Accuracy (%)	Kappa coefficient	Water Area(km²)	Relative Error (%)	Overall Accuracy (%)	Kappa coefficient	Water Area(km²)	Relative Error (%)
August, 1994	2308.52	99.99	0.99	2256.27	2.26	-	-	-	-
September,1996	2986.28	88.00	0.74	2820.70	5.54	-	-	-	-
July, 2001	2292.87	96.00	0.91	2252.46	1.76	93.20	0.83	2241.51	2.24
April, 2003	1248.60	93.80	0.86	1240.54	0.65	91.70	0.82	1336.85	7.07
June, 2007	2099.20	90.70	0.81	2044.85	2.59	89.00	0.76	2171.63	3.45
January, 2009	797.17	94.90	0.85	782.87	1.79	88.30	0.72	816.96	2.48
October, 2014	2134.66	95.50	0.90	2062.91	3.36	90.40	0.74	2206.74	3.38
February, 2016	1065.02	89.30	0.75	1095.84	2.89	86.00	0.70	1101.72	3.45
August, 2019	2280.06	91.80	0.81	2204.84	3.30	89.10	0.73	2430.88	6.61

change. Of special importance is the impact of the TGD on the hydrology and ecology of the middle reaches of the Yangtze River. From 1987 to 2002, Dongting Lake was in an expansion state, with the area changes of an upward trend and the increase rate of 67.67km² per year. After the stable storage of the TGD in 2003, the water surface area of Dongting Lake had a more significant downward trend, with a state of degradation. After 2003, the water changes significantly, with a decreasing trend rate of 37.61 km² per year until 2014 year. After 2014, Dongting Lake was in a stable and recovery period, with little increasing change in area, which may be related to the Dongting Lake protection policy initiated by the Chinese government in 2014.

Additionally, the climate is also an important factor affecting water surface area changes. Rainfall and temperature are the main climatic factors, which have a complicated relationship with water extent. However, the change in the effect of temperature on the area of a water body is mainly realized by affecting the evapotranspiration and the temperature itself has no direct effect on the area of a water body. Therefore, in Fig. 16, we separately calculated the Pearson correlation between the water area and AP, MP during the whole period. There is a positive correlation between AP, MP, and water area. From the results of the correlation analysis, the correlation between MP and monthly water body area is higher, with a correlation coefficient of 0.43, while the correlation coefficient between AP and annual average water body area is only 0.37. Therefore, monthly-scale data can be used to more clearly analyze the impact of rainfall on the area of water bodies. This also confirms the influence trend of precipitation factor on water body area changes.

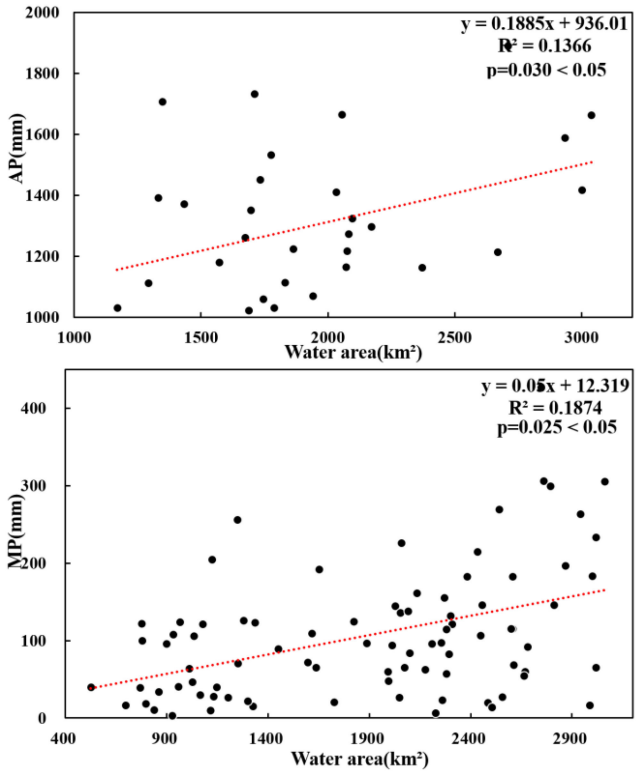

Fig. 16. Pearson correlation coefficient between water area and AP, MP from 1987 to 2020.

C. Comparison With Other Studies in Dongting Lake

We compared the change law of the water extent of Dongting Lake obtained in this study with the results of other researchers, and we found that the change law we obtained was basically the same. For example, the studies by Wu *et al*. [36], Yang *et al*. [37], and Huang *et al*. [30] showed that in recent years, more than a decade, the water area of Dongting Lake has shown a clear downward trend, especially since the establishment of the TGD. Likewise, the water area of Dongting Lake showed obvious seasonal variation characteristics, and the water area change in the dry and wet seasons was more obvious. In addition, the phased method of this study was more scientifically effective on the GEE platform, as it was more convenient to explore the laws for water surface extent change through different time scales for SDG 6.6.1. The most important thing is that we divided the change in the water area of Dongting Lake into three stages and deeply analyzed the temporal and spatial characteristics of the water area of Dongting Lake. So far, most studies on Dongting Lake have used a traditional water body index threshold method to extract water surface, such as NDVI, NDWI, and AWEI, and did not reveal the dynamic temporal and spatial characteristics of the water body of Dongting Lake, and the time scale they studied was small, which was not enough to reflect the change

in the water area of Dongting Lake on a longer time scale [30], [36], [37]. They only analyzed the overall change of the water area of Dongting Lake and did not study the change in the water body at different time scales in detail. In this study, we used the MIWDR method to extract the water surface quickly and accurately. Moreover, the image processing and water extraction process on the GEE platform has a higher extraction efficiency and result analysis for SDG 6.6.1 in this study.

D. Limitations and Prospects

There are still some limitations to this study.

1) There is an issue of data source processing. Although Landsat data have the advantage of spatial resolution, time series, the revisit period is long, which brings great challenges to the high-frequency extraction of water surface area. In addition, Landsat data are easily affected by clouds, fog, and snow and affects the extraction of the water body. In this study, we processed 783 images, but we only retained 89 scenes of effective data, which do not truly reflect the specific change characteristics of Dongting Lake, which also leads to our research on the spatial and temporal characteristics of Dongting Lake being not completely accurate.

2) In terms of water body verification, this study selected nine images of different periods from the 89 effective water body extraction images for verification. The selected verification images are still relatively small, which may affect the accuracy verification of the water body extraction results. (3) The analysis of the influencing factors of the water surface change characteristics of Dongting Lake is not detailed enough. In this study, we only collected precipitation data to analyze its impact on the water body area. Due to the difficulty of obtaining hydrological data in the Dongting Lake area and the complexity of climate and human activities in the area, this study did not collect more data sets for a comprehensive analysis of the driving forces of the water body area.

In the future study, first, we will conduct a quantitative analysis on the influencing factors of the Dongting Lake water body, not just qualitative analysis. We also need to add multifactor analysis to better explore the influencing factors of the Dongting Lake water body. We need to optimize the processing of the data source and introduce multiple remote sensing data sources to analyze the water body of Dongting Lake, such as Sentinel, HJ, and other high-resolution data. We can increase the effectiveness and long-term nature of the remote sensing data, which will be beneficial to our multidata coupling analysis process. Therefore, we can better perform long-time high-frequency water extent extraction in Dongting Lake for SDG 6.6.1 and analyze the causes of changes in the water body of Dongting Lake more comprehensively.

V. Conclusion

In this study, to monitor SDG 6.6.1 indicator, we used Landsat images and new MIWDR to extract the water extent of Dongting Lake from 1987 to 2020. Finally, the dynamic spatiotemporal change of Dongting Lake was analyzed quickly and accurately. The conclusion drawn by this study mainly includes the following:

1) The long time series water extent change of Dongting Lake had obvious fluctuation characteristics. Based on SDG 6.6.1, the maximum water extent was 3060.30 km², which occurred in 1998, and the minimum was 524.09 km² in 2014. The mean water area of Dongting Lake was 1858.38 km² from 1987 to 2020.
2) The monthly water extent of Dongting Lake exhibited inter-annual changes characteristics based on SDG 6.6.1. For the monthly mean water extent, the largest water extent was 2477.14 km² (July) and the smallest was 848.14 km² (January). The water extent varied greatly between the wet and dry seasons. The monthly mean water extent in the wet season mostly exceeded 2000 km², while that in the dry season was mostly less than 1500 km², and most was less than 1000 km².
3) The water extent of Dongting Lake had obvious seasonal changes characteristics. Among the seasonal mean area, summer was the largest at 2438.06 km², and winter was the smallest at 967.34 km². The water extent in summer and autumn was obviously higher than that in spring and winter. The water extent of all seasons showed a downward trend in general, with the fastest decline in spring.
4) The yearly water extent changes of Dongting Lake showed a trend of first increasing and then decreasing and stabilizing. We divided the annual water body of Dongting Lake into three stages. In the annual mean water extent, the largest area was 3038.74 km², which was in 1998, and the smallest area was 1168.74 km², which was in 2008.
5) In the WIF of Dongting Lake, the seasonal water body accounted for the highest proportion, indicating that the Dongting Lake water extent exhibited obvious seasonal characteristics from 1987 to 2020. The permanent water area was 1086.21 km², accounting for 33.56%. The seasonal water area was 1577.85 km², which accounted for 48.74%, and the nonwater area was 573.02 km², which accounted for 17.70%.

Additionally, we also assessed the water extraction accuracy and possible factors for water changes. In short, the overall trend of the water extent change of Dongting Lake from 1987 to 2020 was a downward trend, which was characterized by obvious seasonal changes, and there was a large difference between different periods, which was consistent with the results of our analysis of different time scales and spatial distribution characteristics of the analysis of the inundation frequency of Dongting Lake for SDG 6.6.1. However, due to the limitations and uncertainty of our study, we need to further investigate the factors that affect the water extent of Dongting Lake in the follow-up research, to go deeper into the extent changes of Dongting Lake and promote our protection and management of regional water resources to realize the SDG 6.6.1 indicator.

References

[1] E. Fitoka *et al.*, "Water-related ecosystems' mapping and assessment based on remote sensing techniques and geospatial analysis: The SWOS national service case of the greek ramsar sites and their catchments," *Remote Sens. Environ.*, vol. 245, Aug. 2020, Art. no. 111795.

[2] UN Water, "Progress on water-related ecosystems: Piloting the monitoring methodology and initial findings for SDG indicator 6.6.1," pp. 807–3712, 2018.

[3] C. J. Vörösmarty *et al.*, "Global water resources: Vulnerability from climate change and population growth," *Science*, vol. 289, no. 5477, pp. 284–288, Jul. 2000.

[4] Z. M. Subin *et al.*, "An improved lake model for climate simulations: Model structure, evaluation, and sensitivity analyses in CESM1," *J. Adv. Model. Earth Syst.*, vol. 4, no. 1, Jan-Mar. 2012.

[5] M. A. Holgerson *et al.*, "Large contribution to inland water CO 2 and CH 4 emissions from very small ponds," *Nature Geosci.*, vol. 9, no. 3, pp. 222–226, Feb. 2016.

[6] P. Rao *et al.*, "Dynamic change analysis of surface water in the Yangtze River Basin based on MODIS products," *Remote Sens.*, vol. 10, no. 7, Jun. 2018, Art. no. 1025.

[7] C. Prigent *et al.*, "Changes in land surface water dynamics since the 1990s and relation to population pressure," *Geophys. Res. Lett.*, vol. 39, no. 8, Apr. 2012.

[8] R. Adrian *et al.*, "Lakes as sentinels of climate change," *Limnol. Oceanograp.*, vol. 54, no. 6, pp. 2283–2297, Nov. 2009.

[9] L. Feng *et al.*, "Assessment of inundation changes of Poyang lake using MODIS observations between 2000 and 2010," *Remote Sens. Environ.*, vol. 121, pp. 80–92, Jun. 2012.

[10] S. E. Hampton *et al.*, "Sixty years of environmental change in the world's largest freshwater lake–Lake Baikal, Siberia," *Glob. Change Biol.*, vol. 14, no. 8, pp. 1947–1958, Aug. 2008.

[11] B. Lennox *et al.*, "Post-glacial climate change and its effect on a shallow dimictic lake in Nova Scotia, Canada," *J. Paleolimnol.*, vol. 43, no. 1, pp. 15–27, Feb. 2010.

[12] H. Gao *et al.*, "On the causes of the shrinking of lake chad," *Environ. Res. Lett.*, vol. 6, no. 3, Aug. 2011, Art. no. 034021.

[13] J. Stevenson *et al.*, "Paoay lake, northern luzon, the philippines: A record of holocene environmental change," *Glob. Change Biol.*, vol. 16, no. 6, pp. 1672–1688, Jun. 2010.

[14] Y. Deng *et al.*, "Long-term changes of open-surface water bodies in the Yangtze River Basin based on the google earth engine cloud platform," *Remote Sens.*, vol. 11, no. 19, Sep. 2019, Art. no. 2213.

[15] C. Wang *et al.*, "Long-term surface water dynamics analysis based on landsat imagery and the google earth engine platform: A case study in the middle Yangtze River Basin," *Remote Sens.*, vol. 10, no. 10, Oct. 2018, Art. no. 1635.

[16] L. Kumar and O. Mutanga, "Google earth engine applications since inception: Usage, trends, and potential," *Remote Sens.*, vol. 10, no. 10, Sep. 2018, Art. no. 1509.

[17] A. J. Oliphant *et al.*, "Mapping cropland extent of southeast and northeast asia using multi-year time-series landsat 30-m data using a random forest classifier on the Google Earth Engine cloud," *Int. J. Appl. Earth Observ. Geoinf.*, vol. 81, pp. 110–124, 2019.

[18] J.-F. Pekel *et al.*, "High-resolution mapping of global surface water and its long-term changes," *Nature*, vol. 540, no. 7633, pp. 418–422, Dec. 2016.

[19] Z. Zou *et al.*, "Divergent trends of open-surface water body area in the contiguous united states from 1984 to 2016," *Proc. Nat. Acad. Sci.*, vol. 115, no. 15, pp. 3810–3815, Mar. 2018.

[20] Y. Zhou *et al.*, "Continuous monitoring of lake dynamics on the Mongolian Plateau using all available Landsat imagery and Google Earth Engine," *Sci. Total Environ.*, vol. 689, pp. 366–380, Nov. 2019.

[21] F. Yao *et al.*, "Constructing long-term high-frequency time series of global lake and reservoir areas using Landsat imagery," *Remote Sens. Environ.*, vol. 232, Oct. 2019, Art. no. 111210.

[22] K. Jia *et al.*, "Spectral matching based on discrete particle swarm optimization: A new method for terrestrial water body extraction using multi-temporal Landsat 8 images," *Remote Sens. Environ.*, vol. 209, pp. 1–18, May 2018.

[23] Y. Deng *et al.*, "Spatio-temporal change of lake water extent in Wuhan urban agglomeration based on Landsat images from 1987 to 2015," *Remote Sens.*, vol. 9, no. 3, Mar. 2017, Art. no. 270.

[24] X. Wang *et al.*, "Analysis of the dynamic changes of the Baiyangdian lake surface based on a complex water extraction method," *Water*, vol. 10, no. 11, Nov. 2018, Art. no. 1616.

[25] M. G. Tulbure *et al.*, "Surface water extent dynamics from three decades of seasonally continuous landsat time series at subcontinental scale in a semi-arid region," *Remote Sens. Environ.*, vol. 178, pp. 142–157, Jun. 2016.

[26] S. K. McFeeters, "The use of the normalized difference water index (NDWI) in the delineation of open water features," *Int. J. remote Sens.*, vol. 17, no. 7, pp. 1425–1432, May 1996.

[27] H. Xu, "Modification of normalised difference water index (NDWI) to enhance open water features in remotely sensed imagery," *Int. J. Remote Sens.*, vol. 27, no. 14, pp. 3025–3033, Jul. 2006.

[28] G. L. Feyisa *et al.*, "Automated water extraction index: A new technique for surface water mapping using Landsat imagery," *Remote Sens. Environ.*, vol. 140, pp. 23–35, Jan. 2014.

[29] J. Li *et al.*, "Sedimentation effects of the Dongting lake area," *J. Geographical Sci.*, vol. 19, no. 3, pp. 287–298, Jul. 2009.

[30] S. Huang *et al.*, "Water surface variations monitoring and flood hazard analysis in Dongting lake area using long-term Terra/MODIS data time series," *Natural Hazards*, vol. 62, no. 1, pp. 93–100, 2012.

[31] F. Li *et al.*, "Spatial risk assessment and sources identification of heavy metals in surface sediments from the Dongting lake, Middle China," *J. Geochem. Explor.*, vol. 132, pp. 75–83, Sep. 2013.

[32] J. Wang *et al.*, "Monitoring decadal lake dynamics across the Yangtze basin downstream of Three Gorges Dam," *Remote Sens. Environ.*, vol. 152, pp. 251–269, Sep. 2014.

[33] Y. Du *et al.*, "Lake area changes in the middle Yangtze region of China over the 20th century," *J. Environ. Manage.*, vol. 92, no. 4, pp. 1248–1255, Apr. 2011.

[34] X. Ding and X. Li, "Monitoring of the water-area variations of Lake Dongting in China with ENVISAT ASAR images," *Int. J. Appl. Earth Observ. Geoinf.*, vol. 13, no. 6, pp. 894–901, Dec. 2011.

[35] F. Deng *et al.*, "Analysis of the relationship between inundation frequency and wetland vegetation in Dongting lake using remote sensing data," *Ecohydrology*, vol. 7, no. 2, pp. 717–726, Apr. 2014.

[36] G. Wu and Y. Liu, "Mapping dynamics of inundation patterns of two largest river-connected lakes in China: A comparative study," *Remote Sens.*, vol. 8, no. 7, Jun. 2016, Art. no. 560.

[37] L. Yang *et al.*, "Four decades of wetland changes in Dongting Lake using Landsat observations during 1978-2018," *J. Hydrol.*, vol. 587, Aug. 2020, Art. no. 124954.

[38] Y. Xie *et al.*, "The impact of Three Gorges Dam on the downstream eco-hydrological environment and vegetation distribution of East Dongting Lake," *Ecohydrology*, vol. 8, no. 4, pp. 738–746, Jun. 2015.

[39] X. Lai *et al.*, "Effects of the normal operation of the Three Gorges Reservoir on wetland inundation in Dongting Lake, China: A modelling study," *Hydrological Sci. J.*, vol. 58, no. 7, pp. 1467–1477, Oct. 2013.

[40] G. Wu and Y. Liu, "Capturing variations in inundation with satellite remote sensing in a morphologically complex, large lake," *J. Hydrol.*, vol. 523, pp. 14–23, Apr. 2015.

[41] Y. Cai *et al.*, "Monitoring the vegetation dynamics in the Dongting Lake Wetland from 2000 to 2019 using the BEAST algorithm based on dense Landsat time series," *Appl. Sci.*, vol. 10, no. 12, Jun. 2020, Art. no. 4209.

[42] Y. Xu, W. Liu, J. Song, L. Yao, and S. Gu, "Dynamic monitoring of the lake area in the middle and lower reaches of the Yangtze river using MODIS images between 2000 and 2016," *IEEE J. Sel. Topics Appl. Earth Observ. Remote Sens.*, vol. 11, no. 12, pp. 4690–4700, Dec. 2018.

[43] Y. Yuan *et al.*, "Variation of water level in Dongting Lake over a 50-year period: Implications for the impacts of anthropogenic and climatic factors," *J. Hydrol.*, vol. 525, pp. 450–456, Jun. 2015.

[44] W. Jiang *et al.*, "Analysis of vegetation response to rainfall with satellite images in Dongting Lake," *J. Geographical Sci.*, vol. 21, no. 1, pp. 135–149, Mar. 2011.

[45] D. Peng *et al.*, "Study of Dongting Lake area variation and its influence on water level using MODIS data," *Hydrol. Sci. J.*, vol. 50, no. 1, Feb. 2005.

[46] Y. Long *et al.*, "Estimating real-time water area of Dongting Lake using water level information," *Water*, vol. 11, no. 6, Jun. 2019, Art. no. 1240.

[47] H. B. Mann, "Nonparametric tests against trend," *Econometrica*, vol. 13, no. 3, pp. 245–259, Jul. 1945.

[48] M. G. Kendall, *Rank Correlation Methods*, Oxford, UK: Griffin, 1948.

[49] Z. Jiang *et al.*, "Surface water extraction and dynamic analysis of Baiyangdian Lake based on the Google Earth Engine platform using sentinel-1 for reporting SDG 6.6.1 indicators," *Water*, vol. 13, no. 2, Jan. 2021, Art. no. 138.

[50] Pickens, A. H. *et al.*, "Mapping and sampling to characterize global inland water dynamics from 1999 to 2018 with full Landsat time-series," *Remote Sens. Environ.*, vol. 243, Apr. 2020, Art. no. 111792.

Chunlin Wang received the B.S. degree from Zhengzhou University, Zhengzhou, China. He is currently working toward the Master's degree at Beijing Normal University, Beijing, China, mainly engaged in remote sensing of water resource and environment.

Weiguo Jiang received the B.S. degree from Hunan Normal University, Changsha, China, the M.S. degree from Nanjing Normal University, Nanjing, China, and the Ph.D. degree from Beijing Normal University, Beijing, China.

He is currently a Professor with Beijing Normal University. His research interests include remote sensing, hydrology and International urban wetland protection, and exploration of SDGs.

Yue Deng received the B.S. degree in GIS from Southwest University, Chongqing, China. He is currently working toward the Ph.D. degree at Beijing Normal University, Beijing, China.

He conducted research at University of Nebraska-Lincoln (UNL), as a joint Ph.D. student from 2018 to 2019. His research is focused on water surface mapping using multiple-source remote sensing data.

Ziyan Ling received the B.S. degree from Nanjing Forestry University, Nanjing, China, in 2008, and the M.S. degree from Beijing Normal University, Beijing, China, in 2011, where she is currently working toward the Ph.D degree in cartography and GIS.

She is engaged in 3S teaching and scientific research in Nanning Normal University.

Yawen Deng received the B.S. degree in geographic information science, in 2020 from Beijing Normal University, Beijing, China, where she is currently working toward the Master's degree.

Her research interests include ecohydrographic and wetland remote sensing.